Arabian Journal of Chemical and Environmental Research

Vol. 10 Issue 1 (2023) 1–16

Thermodynamic and Equilibrium Evaluation for Anionic Dye Adsorption using Utilized Biomass-based Activated Carbon: Regeneration and Reusability Studies

M. Husaini[1]* B. Usman[2] and M. B. Ibrahim[3]

[1]*Department of Pure and Industrial Chemistry, Faculty of Physical Sciences College of Natural and Pharmaceutical Sciences, Bayero University Kano (BUK), P.M.B. 3011, Kano, Nigeria.*
[2]*Department of Pure and Industrial Chemistry, Faculty of Physical Sciences College of Natural and Pharmaceutical Sciences, Bayero University Kano (BUK), P.M.B. 3011, Kano, Nigeria.*
[3]*Department of Pure and Industrial Chemistry, Faculty of Physical Sciences College of Natural and Pharmaceutical Sciences, Bayero University Kano (BUK), P.M.B. 3011, Kano, Nigeria.*

[2] *busman.chm@buk.edu.ng* ; [3] *mbibrahim.chm@buk.edu.ng*

Received 01 March 2023, Revised 21 Apr 2023, Accepted 24 Apr 2023

Abstract

Textile wastewater contains harmful dyes that cannot be denied, making them a significant concern for both the economy and human health. To address the efficient removal of these dyes, various adsorbents inspired by nature have been used. This study, utilized black plum seed shell activated carbon (BPAC) as a new, highly effective, inexpensive, and readily available adsorbent for the uptake of methyl orange dye. Several experiments were conducted to study the effect of experimental factors using batch adsorption methods. Scanning Electron Microscopy and Fourier Transform Infrared Spectroscopy (FT-IR) and pH at point of zero charge (pH_{pzc}) were employed to examine the surface characteristics of the BPAC. The well-fitted Freundlich models (R^2 = 0.9956) confirmed that the adsorption process on the BPAC surface followed a heterogeneous multilayer mechanism. Thermodynamic parameters ΔS = -0.169 kJ/K, ΔH = -49.05 kJ/mol, and $\Delta G°$ = -3.22, -2.53, -1.84, -1.15 and -4.55 kJ/mol (at 303, 308, 313, 318 and 323 K) indicates feasible exothermic and spontaneous adsorption process. The research on regeneration demonstrated that NaOH solution is more effective in recovering MO from BPAC compared to distilled water, NaCl and HCl solutions. The BPAC was able to be reused five times and maintained an adsorption efficiency of 56.51 %.

Keywords: Adsorption, characterization, kinetics, thermodynamics, regeneration; reusability.

*Corresponding author.
E-mail address: *musahusaini36@gmail.com*

ISSN : 2458-6544

1. Introduction

The textile industry plays a significant role in global economic development. However, one of the challenges associated with textile manufacturing is the discharge of harmful dye waste (Kumar *et al.*,2020). Among various industries, textiles use a large amount of dyes for coloring fibers, resulting in the highest release of dye waste into the environment (Saratale *et al.*, 2020). Approximately 280,000 tons of dyestuff, which accounts for 10%–15% of total dyes used in textile production, are discharged annually (Baysal *et al.*,2020).

Textiles are made up of natural and synthetic fibers and are used to produce various types of clothing. The dyeing, scouring, printing, sizing, mercerizing, de-scouring, bleaching, and finishing processes in textile production contribute to the discharge of wastewater. It is estimated that one ton of natural textiles requires about 60 m^3 of fresh water, while synthetic textiles require approximately 92 m^3, resulting in 17%–20% of wastewater discharges (Yaseen *et al.*, 2019). The limited absorption capacity of fabrics leads to the inefficient adsorption of dye mixtures, resulting in the release of dye waste and abrics can only absorb around 25% of the dye mixture (Chin *et al.*, 2020).

Dyes, which are colored substances, absorb specific wavelengths in the visible spectrum and have stable and complex aromatic structures that are resistant to degradation (Ertugay *et al.*, 2017) [6]. They find applications in various industries such as pharmaceuticals, textiles, cosmetics, food, plastics, photography, and paper production (Yang *et al.*, 2018). Dyes can be classified into synthetic and natural categories, with natural dyes derived from plants or animals. Synthetic dyes are further divided into azo and non-azo dyes, and azo dyes can be categorized as acidic, reactive, basic, vat, disperse, and sulfur dyes (Akartasse *et al.*, 2022). Acidic dye like methyl orange (MO) is commonly used.

Several studies have been published on dye removal methods, which can effectively remove dyes in a short time. These methods can be classified into three major treatment categories: chemical, biological, and physical treatments (Aadouz *et al.*, 2023; Akartasse *et al.*, 2022; Goren *et al.*, 2021; Ofomaja *et al.*, 2019; Salem *et al.*, 2015). Techniques such as advanced oxidation (AOP), electrochemical treatment, adsorption, biological treatment, and membrane filtration are commonly used for dye elimination. Each method has its advantages and disadvantages, but adsorption is the most widely used method due to its ability to remove pollutants at various concentrations (Samsami *et al.*, 2020; Uddin *et al.*, 2011; Husaini *et al.*, 2019a). Therefore, numerous studies have focused on developing efficient and cost-effective adsorbent materials.

Agricultural wastes have been utilized for wastewater treatment due to their easy availability and favorable physicochemical properties, including high adsorption capacity low cost and good removal efficiency. Agricultural wastes mainly contain hemicellulose, lignin, and high molecular weight

cellulose, with small-sized lignocellulosic materials being particularly important for dye removal (Demba *et al.*, 2022; Husaini *et al.*, 2020; Aljeboree *et al.*, 2020; Ad *et al.*, 2016).

Black plum seed shell, is an abundant, cost-effective material with a large surface area, making it a suitable adsorbent for treating textile wastewater. There is limited available information regarding the importance of using Black plum seed shell for the removal of dye wastewater.

The aim of this study is to investigate the possibility of employing Black plum seed shell for removing methyl orange (MO) from textile wastewater. The results demonstrate the potential of Black plum seed shell activated carbon as an adsorbent for eliminating dyes from wastewater.

2. Materials and Methods

2.1. Collection and Preparation of Adsorbent Samples

The adsorbent samples were prepared following the methods described by reference (Husaini *et al.*, 2023a) in which the Gingerbread plum seed shells samples were collected and thoroughly washed with tap water. They were then rinsed extensively with distilled water to eliminate any dust or soluble substances. Subsequently, the seed shells were dried for 72 hours at room temperature in the laboratory until they became crispy. The dried leaves were finely powdered using a mechanical electronic grinder and impregnated with (30%) phosphoric acid solution for 24 hours and dried prior to carbonization. The carbonization took place in a furnace, with a temperature of 400°C, for 2 hours. Following that, the activated samples underwent a washing procedure using distilled water until a neutral solution was achieved. Subsequently, the samples were dried in an oven at 105°C until they reached a constant weight. After drying, the sample was sifted and placed in an airtight container, specifically labeled as BPAC.

2.2. Preparation of Dye Solutions

A stock aqueous solution with a concentration of 1,000 mg L^{-1} was prepared by dissolving 1 g of dye in 1 liter of distilled water. From this stock solution, smaller pollutant solutions of different concentrations were prepared by diluting the stock solution with demineralized water. Hydrochloric acid (HCl) and sodium hydroxide (NaOH) were used to adjust the pH of the different dye solutions during the experiments.

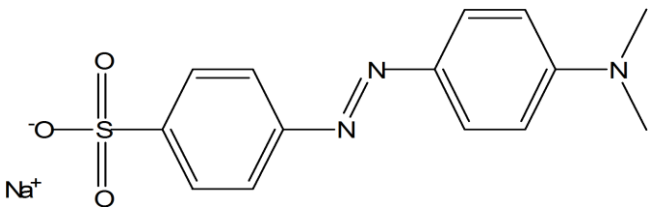

Figure. 1: Structure of Methyl orange

2.3. Batch Adsorption Studies

Batch adsorption experiments were conducted to study the adsorption of MO dyes by BPAC. The experiments involved varying parameters such as agitation time (5 - 150 minutes), adsorbent dosage (0.1 - 500 g), particle size (75 – 900 µm), initial dye concentration (20 - 500 mg/L), and initial dye pH (2-12). The experiments were performed in triplicates at a constant agitation speed of 200 rpm and room temperature (30°C). In each experiment, a specified amount of adsorbent was mixed with 100 cm³ Erlenmeyer flasks containing 50 cm³ of dye solution with a known concentration. The solutions were agitated using an orbital shaker for a specific time period to reach equilibrium. After that, samples were taken out and the supernatant solution was separated from the adsorbent by filtration using Whatman No. 41 filter paper. The initial few drops of the filtrate were discarded. The residual dye concentration in the filtrates was analyzed using a UV-vis spectrophotometer at the respective wavelength of 464.47 nm. The data obtained from triplicate readings were reported as average values. The percentage adsorption and the adsorption capacity of the substrate at equilibrium (mg/g) were calculated using Equations 1 and 2, respectively (Ibrahim *et al.*, 2016).

$$\% \text{ Adsorption} = \frac{C_0 - C_e}{C_0} \times 100 \quad (1)$$

$$qe = \frac{(C_0 - C_e) \times v}{w} \quad (2)$$

In these equations, C_o represents the initial dye concentration in mg/L, Ce represents the concentration at equilibrium or a predetermined time point, V represents the volume of the dye solution used in liters, and w represents the weight of the adsorbent in grams.

2.4. Point of Zero Charge (pH_{pzc})

To determine the pH_{pzc} of the sorbent, Erlenmeyer flasks containing 50 ml of 0.1 M KNO_3 solution were used. The pH of the KNO_3 solutions was adjusted using 0.1 M HCl and NaOH solutions. Next, 0.1 g of the BPAC sorbent was added to the KNO_3 solutions with different pH values. The samples were then shaken for 24 hours. After filtration, the final pH values (pH_f) were measured using a pH meter. The pH_{pzc} value was determined based on the plot of ΔpH as a function of pH_i (Ayuba *et al.*, 2022).

2.5. Fourier Transform Infra-Red (FTIR) Spectroscopy

To gain insights into the surface and structure of the adsorbent and better understand the mechanism of dye binding to adsorbent, FTIR spectroscopy was employed. Both the fresh adsorbent and the adsorbent loaded with dye were subjected to FTIR analysis using a CARY 630 FTIR spectrophotometer manufactured by Agilent Technologies (Husaini *et al.*, 2019b).

2.6. Scanning Electron Microscopy (SEM)

In order to examine the morphology and surface characteristics of the BPAC samples, scanning electron microscopy (SEM) was utilized. The SEM analysis was performed using a Philips XL30 Scanning Electron Microscope with an accelerating voltage of 15kV, a beam size of 3.0, a working distance of 10 and a magnification of 1000. Prior to analysis, the samples were coated with carbon under vacuum conditions to prevent the build-up of static electric charge on the particle surfaces (Husaini *et al.*, 2020).

2.7. Desorption and Recyclability Studies

Batch desorption experiments were conducted using neutral, basic, and acidic desorbing solutions, including distilled water, sodium hydroxide, hydrochloric acid and sodium chloride. To prepare MO - enriched adsorbent, 0.1 g of adsorbent was shaken with 50 cm^3 of a 50 mg/L MO solution at 200 rpm for 90 minutes at 303 K.

In the desorption experiments, the MO - loaded adsorbent was mixed with 50 cm^3 of one of the aforementioned desorbing solutions. The mixture was shaken at 200 rpm for 90 minutes, and the concentration of desorbed dye in the supernatant was analyzed. The effect of desorbing solution concentration was investigated using the eluent that provided the highest dye recovery. A similar procedure was followed with different concentrations (0.1 – 0.5 M) of sodium hydroxide for desorption experiments. The influence of contact time on desorption was also examined using at various time intervals of 5 - 90 minutes (Shahadat *et al.*, 2018). The desorption efficiency was calculated using the following equation 3.

The recyclability of the BPAC was evaluated by performing five successive cycles of adsorption and the amount of adsorbed dye in each cycle was recorded.

$$\text{Desorption efficiency (\%)} = \frac{q_{de}}{q_{ad}} \times 100 \qquad (3)$$

Where, C_{des} and C_{ads} represent the concentrations of desorbed and adsorbed MO in mg/L.

3.0. Results and discussion

3.1. Characterization

FTIR spectra of the adsorbent shown in Figure 2 exhibited notable changes in the observed peaks before and after adsorption, indicating significant alterations in functional groups. The specific functional groups corresponding to these changes can be seen in the Table 1.

SEM is a valuable technique for assessing the properties of adsorbent materials. SEM micrographs of the black plum seed shell activated carbon depicted in Figure 3(a-b) revealed that the powder consisted of fine particles without a defined shape or size. The surface appeared fibrous with irregular macrospores and some enlarged cavities, suggesting the potential for dye molecules to diffuse through the

macrospores of the adsorbent.

The pH at point of zero charge (pH_{pzc}) denotes the pH at which the surface charge of the adsorbent becomes neutral. According to Figure 4, the pH_{pzc} of the BPAC surface is determined to be 5.4. This indicates that at pH 5.4, the cation and anion exchange capacities of the adsorbent are equal. When the pH of the solution exceeds the pH_{pzc}, the surface charge of the adsorbent becomes negative due to proton (H^+) desorption. Conversely, when the pH of the solution is below the pH_{pzc}, the surface charge of the adsorbent becomes positive as a result of the adsorption of positive charges (H^+)

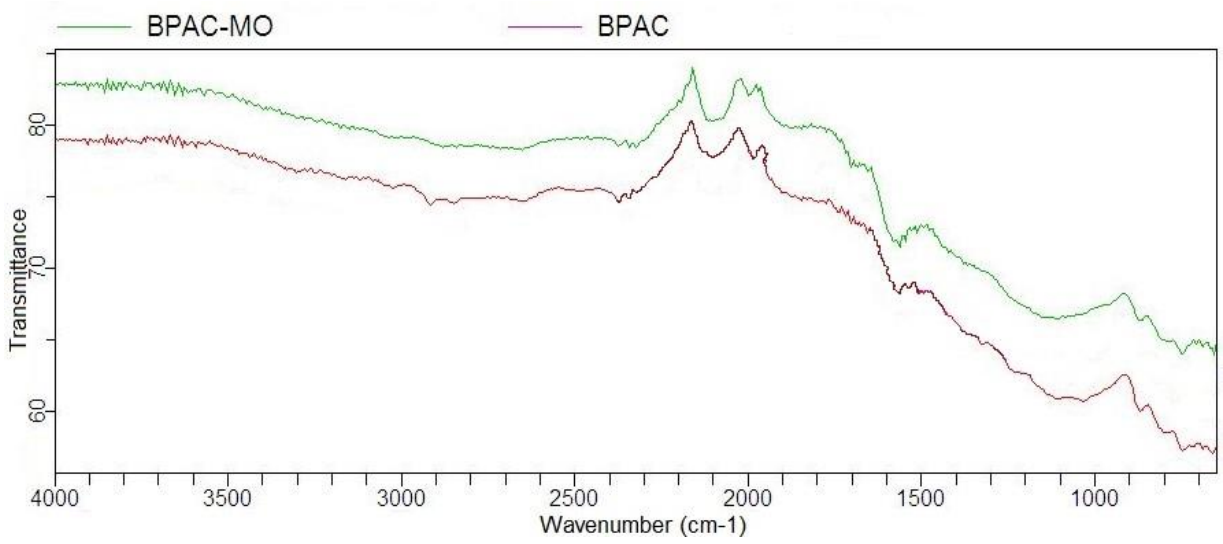

Figure 2. FTIR Spectra of BPAC and BPAC-MO

Table 1. Functional group observed before and after adsorption of MO onto BPAC

Functional group	Wavelength range (cm^{-1})	Before Adsorption	After adsorption
O-H stretching vibration in alcohol	3700-3584	3655	3687
C-H stretching vibration in alkane	3000-2840	2851	2900
C ≡ C stretching vibration in alkyne	2260-2100	2257	2180
C ≡ C stretching vibration in alkyne	2260-2190	2113	2121
C=C=C stretching of allene	2000-1900	1987	1972
C = O stretching of carboxylic acid	1720-1706	1601	1630
N-O stretching of nitro groups	1550-1500	1547	1549
C-H bending of 1,3-disubstituted	880±20	870	879

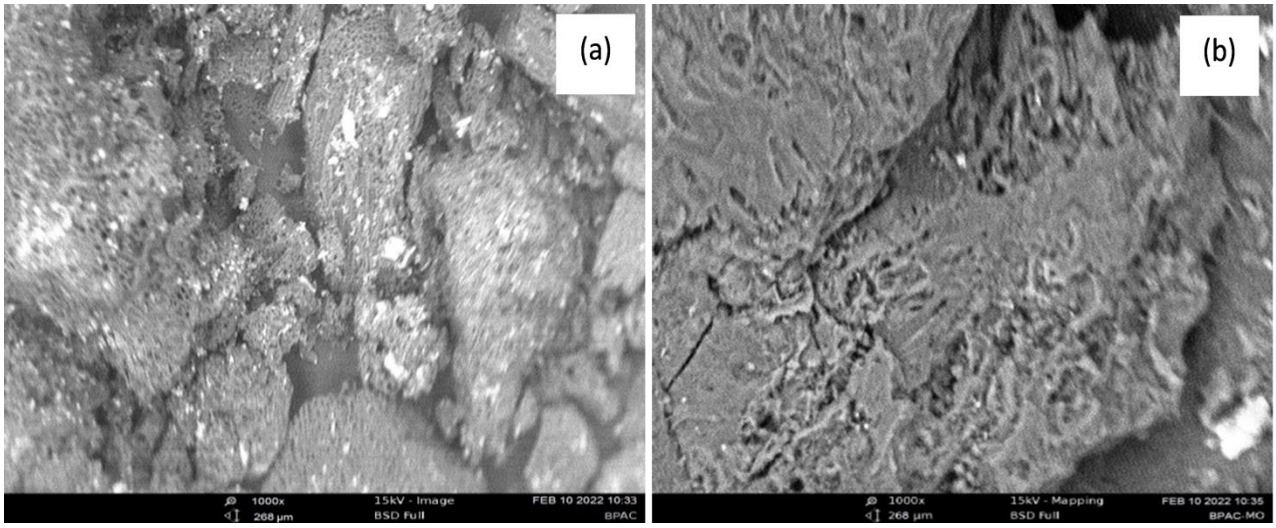

Figure 3. SEM Micrograph (a) BPAC before the adsorption (b) BPAC-MO after the adsorption

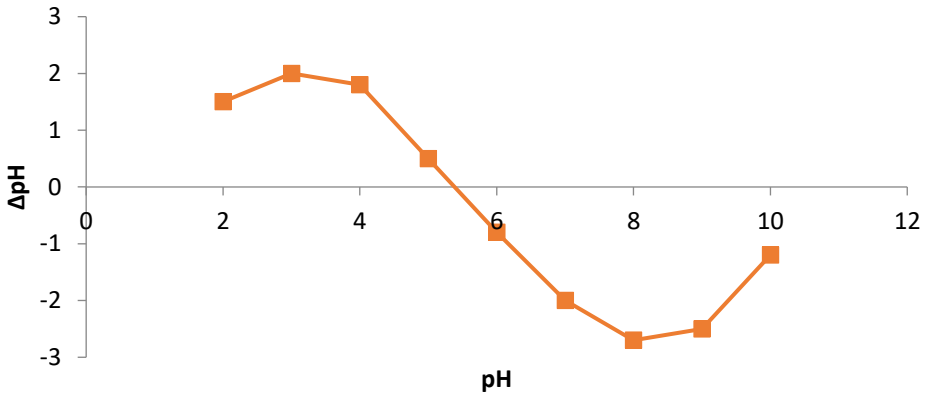

Figure 4. pH at Point of Zero Charge of BPAC

3.2. Batch Adsorption Studies

In The study focusing on batch adsorption and optimization, experiments were conducted to investigate the impact of agitation time (ranging from 5 to 150 minutes) on the percentage of dye adsorption onto the adsorbent. The results (shown in Figure 5a) indicated that the dye adsorption percentage increased rapidly from 45.09 % within the first 5 minutes reaching an optimum level (84.02%) at 60 minutes. Agitation time is a crucial parameter that influences various transfer processes, including adsorption. According to Ibrahim *et al.* (2015), longer agitation time enhances the diffusion rate of dye molecules from the bulk liquid to the liquid-adsorbent interface by increasing turbulence and reducing the thickness of the interphase layer. The initial high dye removal by the adsorbents can be attributed to the availability of numerous vacant sites on the surface for the adsorption of methyl orange.

The impact of adsorbent dosage (ranging from 0.1 to 0.6 g) on the percentage of dye adsorption was investigated at predetermined equilibrium agitation times. The results, illustrated in Figure 5b demonstrate an increase in the percentage of adsorption with an increase in adsorbent dosage, ranging

from 83.89 % to 91.35 %. As the amount of adsorbent increases, the number of active sites available for adsorption also increases, resulting in a higher percentage of dye adsorption. This can be attributed to the presence of accessible sites or surface area on the adsorbents that facilitate the transfer of dyes between the liquid solution phase and the solid phase. At the minimum dosage (0.1 g), there were only a limited number of exchangeable sites available, which led to the removal of minimal amounts of dyes. Conversely, at the maximum dosage (0.5 g), a greater number of exchangeable sites or surface areas were available, leading to the removal of higher amounts of dyes (Yunusa *et al.*, 2021).

Experiments were conducted to investigate the impact of initial concentration of adsorbate (ranging from 20 to 500 mg/L) on the percentage of dye adsorption onto the adsorbent. These experiments were performed at respective equilibrium agitation times, and the finding is depicted in Figure 5c. The percentage of dye adsorption onto the adsorbent exhibited a rapid decrease (from 83.99 to 26.23%) within the concentration range of 20 to 500 mg/L. Conversely, the adsorption capacity of the dye increased with higher concentrations. For a dilute solution (20 mg/L), the amount of dye uptake per unit mass was only 8.40 mg/g. However, in the case of a concentrated solution (500 mg/L), the uptake increased significantly to 65.58 mg/g. These findings clearly indicate that the adsorption process strongly depends on the initial dye concentration.

The surface area of a biosorbent plays a significant role in adsorption, especially when it is higher. As the adsorbent size decreases, the surface area increases, resulting in enhanced adsorption of dye molecules. The percentage of adsorption for methyl orange (85.21% to 35.31% exhibits a notable decrease as the particle size of the adsorbent increases (75µm to 900µm), as shown in Figure 5d This can be explained by the fact that larger particle sizes have a wider diffusion path and reduced total surface area, which hinders the dye's ability to penetrate the internal pore structures of the adsorbents. Conversely, smaller particle sizes have a shorter diffusion path and increased total surface area, enhancing the adsorption ability (Husaini *et al.*, 2023a).

Figure 5e presents the relationship between the amount of MO adsorbed and the pH of the solution. The pH was adjusted from 2 to 12. At lower pH values (higher H^+ concentration), the amount of MO adsorbed per unit mass increased from 92.16 % at pH 2 to 78.21 % mg/g at pH 12. This can be attributed to the positively charged surface of the adsorbents, with pH at point of zero charge (pH_{pzc}) at 5.4. The variation in pH from acidic to alkaline conditions affects both the degree of ionization of the dye molecules and the surface properties of the adsorbents, thereby influencing the rate of dye adsorption. Therefore, conducting adsorption in acidic medium would enhance the positive charge on the adsorbents' surface, leading to increased electrostatic interaction between the anionic MO molecules and the adsorbents' surface, consequently resulting in a higher adsorption rate (Husaini *et al.*, 2023b; Salleh *et al.*, 2011).

Temperature is a crucial parameter in the practical application of adsorption since textile dye effluents are often produced at high temperatures. If the adsorption capacity decreases with increasing temperature, it indicates an exothermic process. Higher temperatures reduce the attractive forces between dye species and the active sites on the adsorbent surface, resulting in lower adsorption quantities (Foo *et al.*, 2012). As shown in Figure 5e the adsorption of methyl orange on BPAC decreased with increasing solution temperature, indicating an exothermic reaction. This suggests that a significant number of molecules gain sufficient energy to interact with the active sites on the surface.

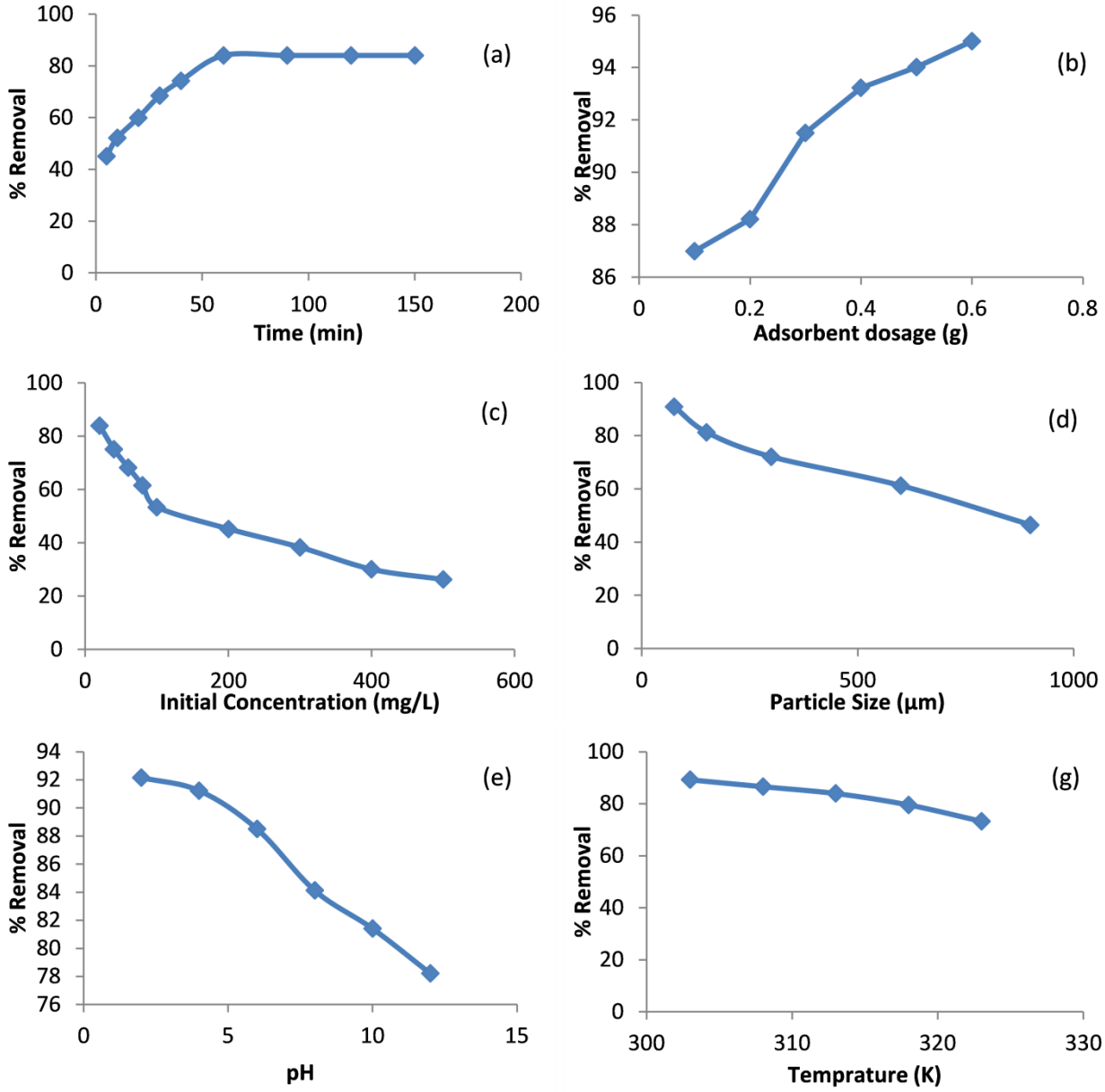

Figures 5. Effect of Various Experimental parameters

3.3 Adsorption Isotherm Models

The isotherm data presented in Table 2 was tested using five commonly used models: Langmuir,

Freundlich, Temkin, and Dubinin-Radushkevich (D-R) models. Based on the linear regression coefficient (R^2) obtained for each model across a wide range of initial concentrations, it was found that the Freundlich model provided the best fit to the data. The order of fit was Freundlich > Langmuir > Temkin > Harkin Jura > D - R. In the case of the Langmuir isotherm, the dimensionless parameter R_L is used to assess the nature of the adsorption process. The heterogeneity factor n_F is employed for the Freundlich isotherm, which represents the deviation from linearity in the adsorption. For the Temkin, Dubinin-Radushkevich (D-R), and Harkins-Jura isotherms, the energy parameters b_T, E, and B_{HJ}, respectively, express the adsorption in terms of its physical or chemical nature (Sharma *et al.*, 2017).

Table 2. Isotherm Parameters for the Adsorption of MO on BPAC

Isotherm Model	Parameters	Values
Langmuir	q_m (mg/g)	48.54
	K_L (L/mg)	0.11
	R_L	0.31
	R^2	0.9274
Freundlich	K_F (mg/g)(L/mg)$^{1/n}$	6.83
	N	2.22
	1/n	0.45
	R^2	0.9935
Temkin	K_T (L/mg)	0.39
	b_T (kJ/mol)	16.35
	R^2	0.8923
D-R	q_m (mg/g)	43.60
	β (mol^{2}k/J^2)	1×10^{-6}
	E (kJ/mol)	0.71
	R^2	0.5043
Harkin Jura	B_{HJ}	2.14
	A	238
	R^2	0.6788

3.4 Thermodynamic Studies

To determine the favorability of the adsorption process, thermodynamic analysis is necessary. Thermodynamic parameters such as the change in Gibbs free energy (ΔG), enthalpy (ΔH), and entropy (ΔS) are involved in assessing the heat change during the adsorption process between the dye and the adsorbent. Experimental investigations conducted at different temperatures provided the values of ΔG,

ΔH, and ΔS using equations 4-6 (Ogata *et al.*, 2018; Ibrahim *et al.*, 2014). Table 3 presents all the thermodynamic parameters.

The decrease in ΔG values indicates that the adsorption of MO on GBAC becomes less favorable as the temperature rises. The negative ΔH value suggests that the sorption process is exothermic and releases energy. Moreover, the negative ΔS value indicates that the solid-solute interface during adsorption becomes less random (Jadhav *et al.*, 2022).

$$K_c = \frac{C_s}{C_e} \quad (4)$$

$$\Delta G = -RT \ln K_c \quad (5)$$

$$ln\ K_c = \frac{\Delta S}{R} - \frac{\Delta H}{RT} \quad (6)$$

The values of ΔH and ΔS were obtained by analyzing the slope and intersection point of the $\ln K_c$ versus 1/T plot. In this context, Cs represents the amount of adsorbate in the adsorbed phase, while Ce indicates the remaining concentration of the dyestuff (in mg/L) in the liquid phase at equilibrium time. T denotes the temperature in Kelvin (K), and R represents the gas constant (8.314 $J \cdot mol^{-1} \cdot K^{-1}$).

Table 3. Thermodynamic Parameters

Temperature (K)	ΔG (kJ/mol)	ΔH (kJ/mol)	ΔS (kJ/K)	R^2
303	-3.22			
308	-2.53			
313	-1.84	-49.05	-0.169	0.9839
318	-1.15			
323	-4.55			

3.5. Regeneration studies

The disposal of exhausted adsorbents can lead to secondary pollution, making it necessary to propose a method for regenerating and reusing the adsorbent. This approach helps reduce the environmental burden associated with sludge disposal. Additionally, valuable adsorbates recovered during regeneration can be used as precursors for the synthesis of important chemicals in industrial processes after appropriate separation (Kankou *et al.*, 2021; Husaini *et al.*, 2023c) (Rabiu *et al.*, 2023). To achieve significant replenishment of the spent adsorbent, various regeneration solutions were evaluated.

Figure 6 shows that the maximum dye recovery (60.0 %) was achieved using sodium hydroxide (NaOH). This can be attributed to the fact that NaOH rises the solution pH, and the OH ions compete favorably with the anionic dye (MO) for the adsorption sites on the adsorbent (BPAC) (Husaini *et al.*, 2023d).

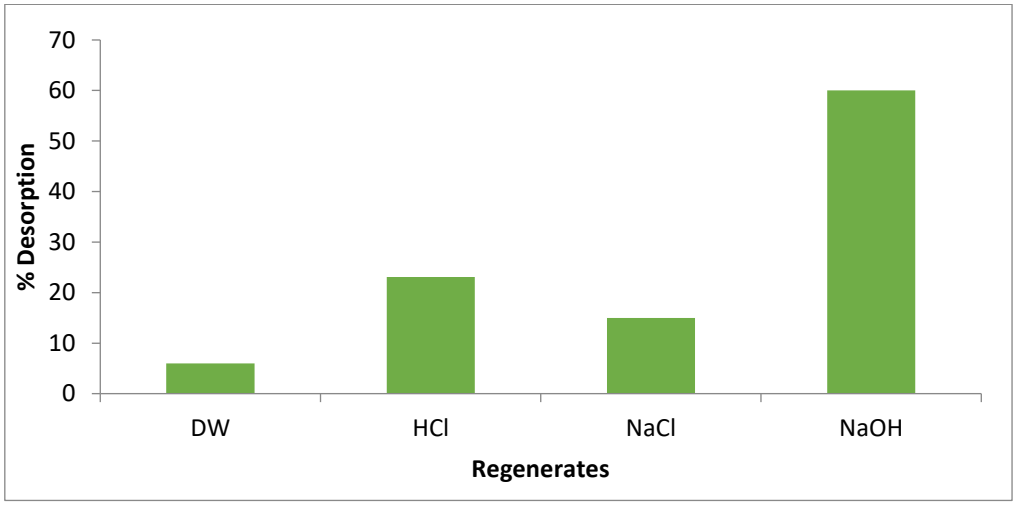

Figure 6. Screening of desorbing solutions

The influence of contact time on MO desorption from the MO-enriched BPAC is shown in Figure 7. It can be observed that the dye was desorbed rapidly within the first 20 minutes and reached maximum elution of 60.51% within 30 minutes. After this initial phase, the percentage recovery remained relatively stable, indicating the attainment of equilibrium in the desorption process.

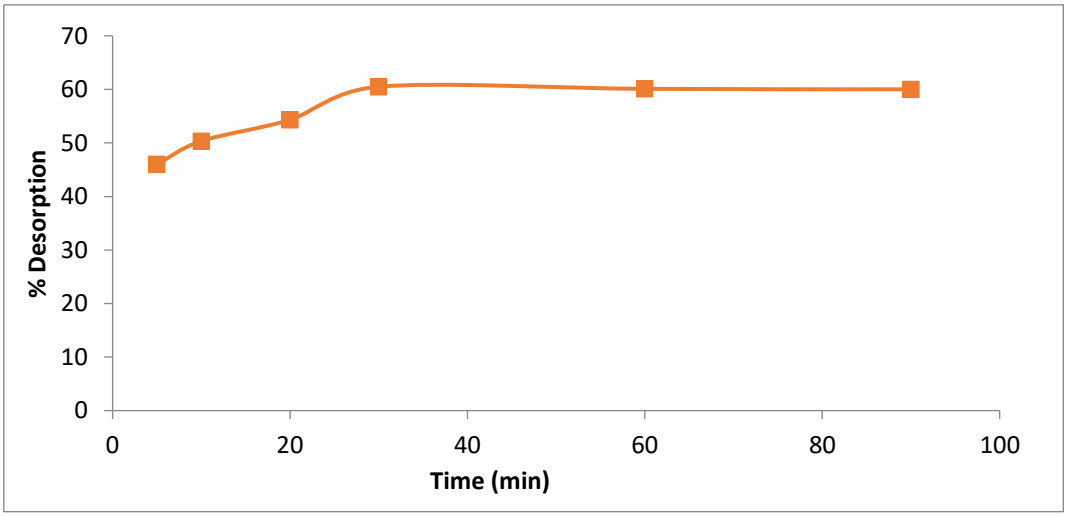

Figure 7. Influence of Contact Time

The concentration of the optimal regeneration solution, NaOH, was also optimized to ensure technical viability for industrial applications. The percentage recovery increased with increasing concentration of NaOH, and a maximum recovery of 60.2 % was achieved using a 0.5 M solution (Figure 8). At higher base concentrations, there were sufficient OH^- ions in the solution to compete with MO on the enriched adsorbent, resulting in higher recovery due to the interference effect.

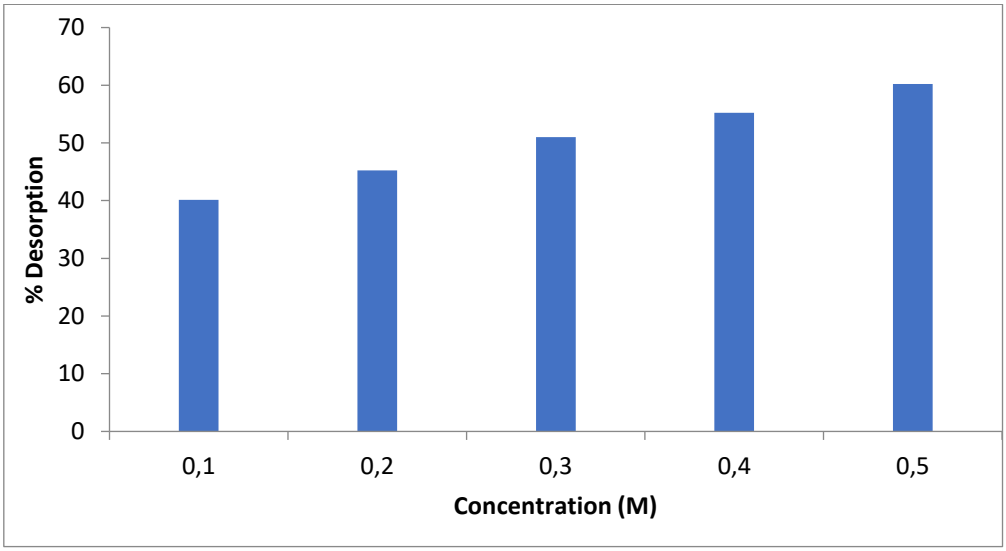

Figure 8. Influence of desorbing solution concentration

The reusability of the adsorbent is an important factor in making adsorption more operationally and economically advantageous (Husaini *et al.*, 2023e). Figure 9 presents the results of the adsorption of MO for five successive cycles. It can be seen that the adsorption efficiency for MO decreased from 84.32 % in the first cycle to 56.51 % in the fifth cycle. This suggests that the adsorbent can be consecutively utilized without significant decline in the adsorption efficacy of MO.

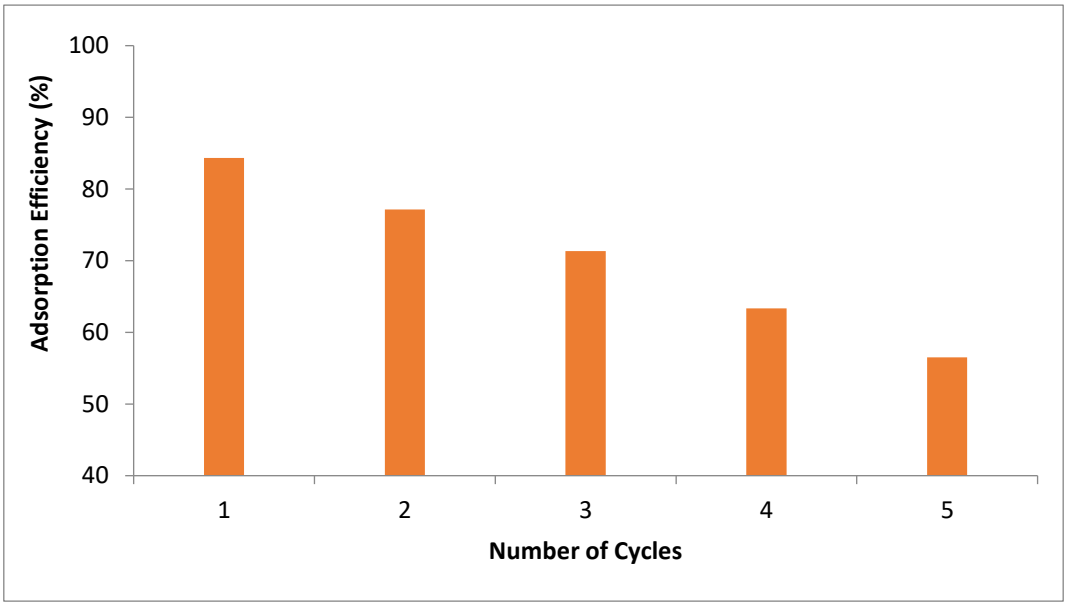

Figure 9. Reusability for successive five adsorption cycles.

Conclusion

This Study suggests a cost-effective method to remove anionic dye (MO), the primary pollutant in textile industries. The effect of different experimental parameters such as contact time, initial dye concentration, adsorbent dosage, particle size, pH and temperature was found to possess a great influence on the adsorption process. The adsorption process was determined to be physisorption, and the experimental

data fit well with Freundlich model. This indicates that the adsorption of MO on gingerbread plum seed shell activated carbon is heterogeneous in nature. Hydrochloric acid served as the best regenerate and the adsorbent was reused in number of five consecutive cycles. Therefore, utilization of black plum seed shell activated carbon as an adsorbent reduces the improper disposal of dyes into the environment.

References

Aaddouz M., Azzaoui K., Akartasse N., Mejdoubi E., Hammouti B., Taleb M., Sabbahi R., Alshahateet S.F. (2023). Removal of Methylene Blue from aqueous solution by adsorption onto hydroxyapatite nanoparticles, *Journal of Molecular Structure*, 1288, 135807, https://doi.org/10.1016/j.molstruc.2023.135807

Ad C., Benalia M., Djedid M., Elmsellem H., Ben Saffedine F., Messaoudi A., Kadmi Y., Ouzidan Y., Hammouti B. (2016), A new lignocellulosic material based on Luffa cylindrica for Nickel(II) adsorption in aqueous solution, *Mor. J. Chem.* 4(4), 1096-1105

Akartasse N., Azzaoui K., Mejdoubi E., Hammouti B., Elansari L.L., Abou-salama M., Aaddouz M., Sabbahi R., Rhazi L. and Siaj M. (2022), Environmental-Friendly Adsorbent Composite Based on Hydroxyapatite/Hydroxypropyl Methyl-Cellulose for Removal of Cationic Dyes from an Aqueous Solution, *Polymers*, 14(11), 2147; https://doi.org/10.3390/polym14112147

Aljeboree A. M., A. N. Alshirifi, and A. F. Alkaim, Highly efficient removal of textile dye 'Direct Yellow (DY12) dyes' from aqueous systems using coconut shell as a waste plants. *Plant Archives.* 20, 1: 3029-3038 (2020).

Ayuba, A. M., Hamza, U., Shurahabil, I. B. and Abdulmumini, H. (2022). Adsorption of Malachite Green Dye Using Carbonized Water Lily Leaves: Kinetics, Equilibrium and Thermodynamics Studies. *UMYU Scientifica*, 1(1), 91-102.

Baysal M., Bilge K., Yılmaz B., Papila M., and Yürüm Y. (2020), Preparation of high surface area activated carbon from waste-biomass of sunflower piths: kinetics and equilibrium studies on the dye removal. *J. Environ. Chem. Eng.*, 6, 2:1702-1713.

Chin J.Y., Chng L.M., and Leong S.S. (2020), Removal of synthetic dye by Chlorella vulgaris microalgae as natural adsorbent. *Arabian J. Sci. Eng.*, 45: 7385-7395.

Demba N'diaye, A., Hammouti, B., Nandiyanto, A. B. D., and Al Husaeni, D. F. (2022). A review of biomaterial As an adsorbent. *Communications in Science and Technology*, 7(1), 140-153.

Ertugay N. and Acar F.N. (2017), "Removal of COD and color from Direct Blue 71 azo dye wastewater by Fenton's oxidation, Kinetic Study," 10, S1158-S1163.

Foo, K. Y., and Hameed, B. H. (2012). Microwave-assisted preparation and adsorption performance of activated carbon from biodiesel industry solid residue: influence of operational parameters. *Bioresource Technology*, 103(1), 398-404.

Goren, M., Murathan, H. B. N., and Murathan, A. M. (2021). Removal of rhodamine B from aqueous solution by using pine cone activated with HNO_3. *J. Int. Environ. Appl. Sc.*,16, 123-132.

Husaini, M. and Ibrahim, M. B. (2019a). Thermodynamic and Kinetics Study on the Corrosion of Aluminum in Hydrochloric Acid Using Benzaldehyde as Corrosion Inhibitor. *International Journal of Engineering and Manufacturing.* 9(6): 53-64.

Husaini, M., Usman, B., Ibrahim, M. B. (2019b). Inhibitive Effect of Glutaraldehyde on the Corrosion of Aluminium in Hydrochloric Acid Solution. *Journal of Science and Technology.* 11(2): 8-16.

Husaini M., Usman B., Ibrahim M.B. (2023a) Competitive Adsorption of Congo red Dye from Aqueous Solution onto Activated Carbon Derived from Black Plum Seed Shell in Single and Multicomponent System. *African Journal of Management and Engineering Technology*, 1(2), 76-89.

Husaini, M., Usman, B., Ibrahim, M. A., and Ibrahim, M. B. (2020). Effect of Aniline as Corrosion inhibitor on the Corrosion of Aluminium in Hydrochloric Acid Solution. *Res. J. Chem. Environ.*, 24(2), 99-106.

Husaini, M., Usman, B., and Ibrahim, M. B. (2023b). Combine Computational and experimental studies for the removal of anionic dyes using activated carbon derive from agricultural waste. *Appl. J. Envir. Eng. Sci.*, 9(4), 245-258

Husaini, M., Usman, B., and Ibrahim, M. B. (2023c). Kinetic and Thermodynamic evaluation on Removal of Anionic Dye from Aqueous Solution using Activated Carbon Derived from Agricultural Waste: Equilibrium and Reusability Studies. *Appl. J. Envir. Eng. Sci*., 9, 124–138.

Husaini, M., Usman, B and Ibrahim, M. B. (2023d). Adsorption Studies of Methylene Blue using Activated Carbon Derived from Sweet Detar Seed Shell. *ChemSearch Journal 14(1): 21 – 32.*

Hussaini, M., Usman, B., and Ibrahim, M. B. (2023e). Modeling and Equilibrium Studies for the Adsorption of Congo red Using Detarium microcarpum Seed Shell Activated Carbon. *Appl. J. Envir. Eng. Sci*., 9, 147–162.

Ibrahim, M. B., and Umar, A. (2016). Adsorption Thermodynamics of Some Basic Dyes Uptake from Aqueous Solution using Albizia lebbeck Shells. *ChemSearch Journal*, 7(1), 43-51.

Jadhav, S. K., and Thorat, S. R. (2022). Adsorption of Azo Dyes Using Biochar Prepared from Regional Crop Waste Material. *Biosciences biotechnology research*, 19(1), 141-151.

Kumar, P., and Kumar, A. J. S. (2020). Research, In silico enhancement of azo dye adsorption affinity for cellulose fibre through mechanistic interpretation under guidance of QSPR models using Monte Carlo method with index of ideality correlation. *SAR and QSAR Environ. Res.*, 31(9), 697-715.

Kankou, M. S. A., N'diaye, A. D., Hammouti, B., Kaya, S., and Fekhaoui, M. (2021). Ultrasound-assisted Adsorption of Methyl Parathion using commercial Granular Activated Carbon from Aqueous solution. *Moroccan Journal of Chemistry*, 9(4), 832-841.

Kumar, D. Y., and Scholz, M. (2019). Textile dye wastewater characteristics and constituents of synthetic effluents: a critical review. *Int. J. Environ. Sci. Technol.*, 16(2), 1193-1226.

N'diaye, A. D., Hammouti, B., Nandiyanto, A. B. D., and Al Husaeni, D. F. (2022). A review of biomaterial As an adsorbent. *Communications in Science and Technology*, 7(1), 140-153.

Ogata, F., Nakamura, T., and Kawasaki, N. (2018). Adsorption capability of virgin and calcined wheat bran for molybdenum present in aqueous solution and elucidating the adsorption mechanism by adsorption isotherms, kinetics and regeneration. *J. Environ. Chem. Eng.*, 6(4), 4459-4466.

Ofomaja, A., Mtshatsheni, K., and Naidoo, E. (2019). Synthesis and optimization of reaction variables in the preparation of pinemagnetite composite for removal of methylene blue dye. S. *Afr. J. Chem. Eng.*, 29(1), 33-41.

Rabiu, M. A., Husaini, M., Usman, B., and Ibrahim, M. B. (2023). Adsorption of Basic Magenta Dye From Aqueous Solution Using Raw And Acid Modified Yam Peel As Adsorbent. 3rd International Conference on Biological, Chemical and Environmental Sciences (BCES-2015),

Sept. 21-22.

Salem S.B. Mezni M., Errami M., Amine K.M., Salghi R., Ali. Ismat H., Chakir A., Hammouti B., Messali M., Fattouch S. (2015), Degradation of Enrofloxacin Antibiotic under Combined Ionizing Radiation and Biological Removal Technologies, *Int. J. Electrochem. Sci.,* 10 N°4, 3613-3622, https://doi.org/10.1016/S1452-3981(23)06565-3

Salleh, M. A. M., Mahmoud, D. K., Karim, W. A., and Idris, A. (2011). Cationic and anionic dye adsorption by agricultural solid wastes: a comprehensive review. *Desalination,* 280, 1-13.

Saratale, R. G., Banu, J. R., Shin, H.-S., Bharagava, R. N., and Saratale, G. D. (2020). Textile Industry Wastewaters as Major Sources of Environmental Contamination: Bioremediation Approaches for its Degradation and Detoxification, in Bioremediation of Industrial Waste for Environmental Safety. *Springer,* 135-167.

Samsami, S., Mohamadizaniani, M., Sarrafzadeh, M. H., Rene, E. R., and Firoozbahr, M. (2020). Recent advances in the treatment of dye-containing wastewater from textile industries: overview and perspectives. *Process Saf. Environ. Protect*, 143, 138-163.

Shahadat, M., and Ismail, S. (2018). Regeneration performance of clay-based adsorbents for the removal of industrial dyes: a review. *RSC advances*, 8(43), 24571-24587.

Sharma, K., Vyas, R. K., and Dalai, A. K. (2017). Thermodynamic and kinetic studies of methylene blue degradation using reactive adsorption and its comparison with adsorption. *J. Chem. Eng. Data*, 62(11), 3651-3662.

Uddin, M. J., Ampiaw, R. E., and Lee, W. (2011). Adsorptive removal of dyes from wastewater using a metal-organic framework: a review. *Chemosphere,* 284, 131314.

Yunusa, U., Husaini, M., Ibrahim, A. K., Abdullahi, Y., and Abdullahid, T. (2021). Hexavalent chromium removal from simulated wastewater using biomass-based activated carbon. *Algerian Journal of Engineering and Technology*, 04, 030–044.

Yaseen, D., and Scholz, M. (2019). Textile dye wastewater characteristics and constituents of synthetic effluents: a critical review. *Int. J. Environ. Sci. Technol.*, 16(2), 1193-1226.

Yang, L., Chen, J., and Qin, S. (2018). Growth and lipid accumulation by different nutrients in the microalga Chlamydomonas reinhardtii. *Biotechnol. Biofuels.* 11(1), 40.